Journal of Materials Chemistry A

Accepted Manuscript

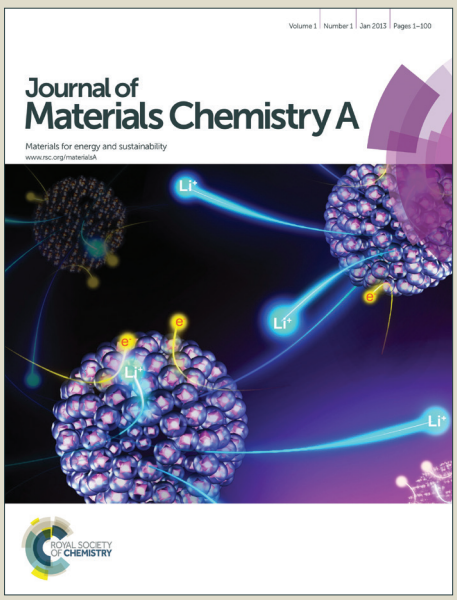

ROYAL SOCIETY OF CHEMISTRY

www.rsc.org/materialsA

Comprehensive strategy to design highly ordered mesoporous Nafion membranes for fuel cells under low humidity conditions

Jin Zhang[1], Junrui Li[2,3], Haolin Tang[2,*], Mu Pan[2] and San Ping Jiang[1,*]

[1]Fuels and Energy Technology Institute & Department of Chemical Engineering, Curtin University, Perth, WA 6102, Australia

[2]State Key Laboratory of Advanced Technology for Materials Synthesis and Processing, Wuhan University of Technology, Wuhan 430070, China

[3]Department of Chemistry, Wuhan University of Technology, Wuhan 430070, China

Abstract: A comprehensive strategy has been developed to synthesize highly ordered mesoporous Nafion membranes with different structure symmetries including 2D hexagonal (2D-H), 3D face-centered (3D-FC), 3D cubic-bicontinuous (3D-CB) and 3D body-centered (3D-BC), using a soft template method with the assistance of silica colloidal mediator. The Nafion membrane derived from the self-assembled mesoporous Nafion-silica composites maintained the microstructures of the silica framework, which was confirmed by the small angle X-ray scattering (SAXS) and TEM. The *in situ* time-resolved synchrotron SAXS clearly indicates that the presence of silica colloids is critical for the formation of the highly ordered mesoporous structured phase in the precursor solution. The best results are observed on Nafion membranes with 2D-H structure in terms of proton conductivity and cell performance under reduced relative humidity (RH) conditions, achieving proton conductivity of 0.08, 0.062 and 0.038 S cm^{-1} at 100, 40 and 0%RH, respectively. Moreover, the power

Jin Zhang and Junrui Li contribute equally to this paper.

Corresponding author. tanghaolin2005@yahoo.com.cn (H. L. Tang), s.jiang@curtin.edu.au (S. P. Jiang)

output of the mesoporous Nafion membrane cells show a S-shaped dependence on RH and is stable under anhydrous conditions (i.e., 0% RH), demonstrating an outstanding high water retention capability of the mesoporous structure of the membranes.

Keywords: Proton exchange membrane fuel cells; highly ordered mesoporous Nafion; synchrotron SAXS; ordered mesoporous structure formation; anhydrous conditions.

1 Introduction

Nafion membrane is the state-of-the-art proton exchange membrane (PEM) because of its high proton conductivity in fully hydrated state, good mechanical property, chemical stability and structural integrity.[1-3] However, the high dependence of the proton mobility in Nafion membrane on relative humidity (RH) requires the high level of RH for the stable operation of Nafion membrane based fuel cells, which not only complicates the water management but also increases the cost.[4] The high sensitivity of Nafion membranes to RH is mainly due to the fact that Nafion membrane has a non-ordered nanostructure consisting of hydrophobic perfluorinated main chains surrounded by hydrophilic ionic domains that swell upon hydration.[5-7] The growth of ionic domains during the water sorption induces a phase-separation, where water-swollen ionic domains tend to interconnect nanochannels and thus facilitate water and ion transport through the hydrophobic polymer matrix.[8] However, the water channels in Nafion membrane are random, which results in the inherent limitation in the relatively low water retention ability of conventional Nafion membrane.[9]

We have shown early that mesoporous structures can be introduced into the Nafion membrane via a soft template method.[10, 11] In this method, a nonionic block copolymer surfactant, PEO_{127}-PPO_{48}-PEO_{127} (Pluronic F108) was introduced during the formation of Nafion membranes and the surfactant embedded in the synthesized Nafion membranes is removed by reflux with hot water, forming mesoporous structures in Nafion. The mesoporous Nafion membranes synthesized by solft template method show higher water retention and proton conductivity than pristine Nafion membrane due to vapor condensation effect within the confined space of mesoporous channels.[11-13] However, the degree of order of the mesoporous structure is rather low because it is difficult to form highly ordered micelles in the solution due to the flexible nonionic block polymer chains. This is indicated by the low resolved and broad SAXS peak of as-synthesized mesoporous Nafion.[11] In order to significantly increase the long-range periodic and ordered mesoporous structures, we employed silica colloidals as mediator in addition to nonionic surfactant to facilitate the formation of highly ordered mesoporous Nafion membranes.[14] The presence of silica colloidal mediator significantly increased the degree of order of mesoporous structure of Nafion membrane. However, the formation of mesoporous Nafion nanostructure and the interactions between nonionic block copolymer surfactant, silica colloidal and Nafion inomers are largely unknown although the formation of mesoporous silica materials *via* the nonionic block polymer template has been extensively studied.[15-17]

Therefore, fundamental understanding of the interaction among nonionic block copolymer micelles, Nafion ionomers and silica precursor is of scientific and

technological importance in order to optimize the structure and proton conductivity properties of PFSA-based membranes like Nafion for fuel cells application. On the other hand, although the presence of ordered mesoporous structure in Nafion membrane enhances the water retention and proton conductivity of the membranes under reduced RH,[11] the relationship between the performance of the highly ordered mesoporous Nafion membrane based fuel cells and structural symmetries needs to be identified in order to evaluate the external humidity dependence of the mesoporous Nafion membranes. Consequently, understanding the effect of morphology and microstructure on the proton transportation and the water-retaining capability of Nafion membrane is crucial in the development of efficient Nafion membrane-based energy-conversion and storage devices such as fuel cells and water electrolysis.

Here, small-angle X-ray scattering (SAXS) technique was applied to analyze the microstructures of as-synthesized mesoporous Nafion membranes. Furthermore, we employed *in situ* time-resolved synchrotron SAXS to study the micelles and mesoporous structure formation assisted with silica colloids. The microstructure, mesoporous symmetry, pore size, proton conductivity and performance of the mesoporous Nafion membranes were studied in detail. Cell performance results showed that highly ordered mesoporous Nafion membranes possess substantially high tolerance towards RH fluctuation as compared to the pristine Nafion membranes and can be operated under anhydrous conditions.

2 Experimental

2.1 Materials

All reagents were used as received without further purification. Nonionic triblock copolymers, including poly(ethylene oxide)-*b*-poly(propylene oxide)-*b*-poly-(ethylene oxide) copolymer $EO_{20}PO_{70}EO_{20}$ (Pluronic® P123, MW= 5800, Sigma) and $EO_{106}PO_{70}EO_{106}$ (Pluronic® F127, MW= 12600), tetraethyl orthosilicate (TEOS) and n-butanol (99.4%) were purchased from Sigma-Aldrich. 1,3,5-trimethylbenzene (TMB, 99%), concentrated HCl (AR), HF (40%), KCl (AR) and ethanol (AR) were purchased from Shanghai Chemical Company. Nafion 520 ionomers (EW = 1000, 5 wt %) was purchased from DuPont, USA.

2.2 Synthesis of Nafion membranes with different structure symmetries

Mesoporous Nafion with four different mesoporous structure symmetries, including 2D hexagonal (2D-H), 3D face-centered cubic (3D-FC), 3D body-centered cubic (3D-BC), and 3D cubic-bicontinuous (3D-CB) was synthesized from the Nafion-silica composites. The synthesis procedures for the Nafion-silica composites are as follows:

2D-H Nafion-silica. Typically, 2.0 g of P123 and 10.3 mL concentrated HCl solution were mixed in 62.5 g distilled water. Nafion ionomers was then dropwise added under stirring condition to obtain a homogeneous solution. TEOS (4.16 g) was added and stirred for 24 h. Then the mixture was transferred into an autoclave reactor and kept at 100 ^{o}C for 24 h.

3D-FC Nafion-silica. 2.0 g of F127, 2.0 g of TMB and 5.0 g of KCl were dissolved in HCl solution (2.0 M, 120 mL) under stirring for 24 h. Nafion ionomers was then dropwise added under stirring condition to obtain a homogeneous solution. TEOS (8.3

g) was added and stirred for 24 h. The mixture was transferred into an autoclave reactor and kept at 40 ^{o}C for 72 h.

3D-BC Nafion-silica. 1.07 g of F127 and 2.12 g concentrated HCl were mixed in 51.44 g distilled water. The solution was heated to 45 ^{o}C before adding 3.21 g n-butanol. Nafion ionomers was then dropwise added under stirring condition to obtain a homogeneous solution. TEOS (5.09 g) was added and stirred for 24 h. The mixture was transferred into autoclave reactor and kept at 100 ^{o}C for 24h.

3D-CB Nafion-silica. 2.0 g of P123 and 3.7 g of concentrated HCl solution were mixed to distilled water. The solution was heated to 35 ^{o}C before adding 2.0 g of n-butanol. Nafion ionomers was then dropwise added under stirring condition to obtain a homogeneous solution. TEOS (5.2 g) was added and stirred for 24 h. The mixture was transferred into autoclave reactor and kept at 100 ^{o}C for 24h.

Without specification, Nafion content in the Nafion-silica composites was 10 wt%. Structure directing agents (SDAs), namely triblock copolymers in the as-synthesized Nafion-silica composites as described above, were removed by refluxing in ethanol for 48 h at 70 ^{o}C. Then the Nafion-silica composites were mixed with HF solutions under stirring for 48 h to remove the silica template. Nafion ionomer was isolated and collected by centrifugation treatment at 4000 r min^{-1} for 5 min. Mesoporous Nafion membranes were obtained by recasting the mesoporous Nafion ionomers and heat-treated at 60 ^{o}C for 8 h, 80 ^{o}C for 8 h and then 100 ^{o}C for 2 h.

2.3 Characterization

Small-angle X-ray diffraction (SAXRD) profiles were recorded on a Rigaku D/MAX-RB diffractometer with a CuKα radiation (λ = 1.5419 Å) operating at 40 kV, 50 mA. A linear position-sensitive Dectris-Pilatus detector was used, and the photo energy was 12 keV. Before the test, Nafion-silica composites were grinded finely into powders and the Nafion suspensions were transferred into transparent tubes. Transmission electron microscopy (TEM) was used to characterize the morphology of Nafion by depositing of the Nafion suspension on a lacey carbon grid via electron microscopy (JEOL JEM-2100F) at accelerating voltage of 200 kV. Q500 (TA instrument) Thermogravimetric analyzer was employed to investigate the thermal and water retention of the pristine and mesoporous Nafion membrane samples. The as-prepared membranes were immersed in water at room temperature for 24 h before the test. Then the TGA measurement was conducted from room temperature to 800 ^{o}C with 10 ^{o}C min^{-1} under air flow of 50 SCCM. Nitrogen adsorption isotherms, Brunauer-Emmett-Teller (BET) specific surface areas (S_{BET}) and porosity of the samples were measured at -196 ^{o}C using Micromeritics ASAP 2020 gas adsorption apparatus. Before adsorption measurement the membranes were cut into small pieces and degassed at 100 ^{o}C for 9 h.

The *in situ* time-resolved synchrotron Small-Angle X-ray Scattering (SAXS) measurements were performed with camera length of 650 mm on the Australian synchrotron SAXS beamline with 3 GeV electron storage ring, Melbourne, Australia. The q range was 0.015 – 0.95 Å^{-1}. For mesoporous Nafion-silica composite powders, they were confined in the holes of a flat plate sample holder which were covered with

Kapton tape. The sample plates were then placed on the beamline. In the present study, precursor solution with appropriate compositions of P123, Nafion ionomer and TEOS in HCl solution for 2D-H Nafion-silica composite was selected in the *in situ* time-resolved synchrotron SAXS study. The solution was confined in a transparent homemade apparatus and then it was placed on the sample holder on the beamline. The synchrotron SAXS of solutions was carried out at room temperature without stirring due to the restriction of the sample holder.

2.4. Cell preparation and electrochemical characterization

Pt/C catalysts (50 % Pt/C, E-TEK, USA) were used for the anode and cathode. Pt/C catalyst layer was transferred onto the mesoporous Nafion membrane at 125 ^{o}C and 10 MPa by the decal method to form the catalyst-coated-membrane (CCM). Then CCM was sandwiched between two gas diffusion layers based on Toray® TGP-H-060 carbon paper to form the membrane-electrode-assembly (MEA). The loading for Pt and mesoporous Nafion ionomers in both anode and cathode was 0.2 mg cm^{-2} and 0.4 mg cm^{-2}, respectively. Then the MEA was placed in single-cell hardware (active area 6.25 cm^{-2}) for the cell performance measurement using a Greenlight G20 fuel cell test station. H_2 and O_2 flow rates were 50 mL min^{-1}. The stability of mesoporous Nafion membranes was studied on cells with 2D-H Nafion and Nafion 112 membranes at 60 ^{o}C and different RH under a discharge current density of 100 mA cm^{-2}. Proton conductivity of mesoporous Nafion membranes was measured using electrochemical impedance spectroscopy (EIS) technique at frequencies ranging from 100 KHz to 1

Hz.

Hydrogen crossover across the membrane was evaluated at ambient condition by an electrochemical method. Pure hydrogen and nitrogen (99.9999%) were fed without humidifying to the anode and the cathode, respectively, at 300 mL min^{-1}. The potential of the cathode (in nitrogen) was swept at 2 mV s^{-1} in a potential range of 0 mV to 700 mV against the anode (H_2/H^+) using a voltammetry station (Autolab, PGSTAT30). Hydrogen crossover was evaluated in diffusion-limited hydrogen oxidation current density obtained in the range of 300 – 350 mV.

3 Results and discussion

3.1 Formation and characterization of ordered mesoporous Nafion

The strategy to design highly ordered mesoporous Nafion membrane is based on the co-assembly of Nafion, silica and SDAs to form the onion-like Nafion-silica-SDAs composites.[14] After removal of the SDAs, the Nafion-silica composites show characteristic SAXS diffraction peaks of well-ordered 2D hexagonal (structural symmetry *P6mm*),[18] 3D face-centered cubic (structural symmetry $Fm\overline{3}m$),[19] 3D body-centered cubic (structural symmetry $Im\overline{3}m$)[20] and 3D cubic bicontinuous (structural symmetry $Ia\overline{3}d$)[21] mesoporous silica (as shown in Figure 1A). Moreover, the as-synthesized Nafion membranes after the removal of the mesoporous silica templates show sharp and typical SAXS peaks in the region of q< 0.2 $Å^{-1}$ (Figure 1B), characteristics of the corresponding Nafion-silica mesoporous structure symmetries but with increased intensity. In contrast, pristine Nafion 112

membrane, as the control group, is generally featureless under the present study conditions, indicating that Nafion structure has no long-range and ordered mesopores shown by the SAXS and TEM characterization.[22, 23] The very different SAXS patterns between the mesoporous Nafion and pristine Nafion are also confirmed by the TEM images as well as TGA profile (see Figure 2). The lattice parameter, *a*, of mesoporous Nafion and mesoporous Nafion-silica composites was calculated from SAXS profiles and the data are shown in Table 1. The results indicate that highly ordered mesoporous structures with long-range periodicity remain stable and intact in mesoporous Nafion membranes after the removal of SDA and silica colloids. However, without the assistance of silica colloids, the order degree of the mesoporous structure is much lower, as shown in previous studies.[10, 11] Silica colloids, therefore, plays an important role for the formation of highly ordered mesoporous structured phase in Nafion-SDA-silica precursor solutions with controlled structure symmetries.

Pore size and specific surface area of the mesoporous Nafion membrane were also measured using N_2 adsorption isotherm and the results are shown in Figure 3. Mesoporous Nafion membranes with different symmetries have typical type-IV curves and capillary condensation steps. The 2D-H Nafion shows capillary condensation at relative pressures of 0.55 - 0.8, while typical type-IV curves with a clear condensation step at P/P_0= 0.4 - 0.7 were observed in 3D-FC, 3D-CB and 3D-BC Nafion membranes. The mesoporous Nafion samples generally give the H_1-type hysteresis loop, suggesting the uniform pore sizes distribution and ordered pore shape of the mesoporous Nafion.[24] The mesoporous Nafion shows rather narrow

pore size distributions and the average pore diameter, d_{pore}, is 5.3 nm, 3.8 nm, 3.8 nm and 4.7 nm for 2D-H, 3D-FC, 3D-CB and 3D-BC Nafion, respectively. Based on the d_{pore} and lattice parameter, a (see Table 1), pore wall thickness, d_{wall}, can be calculated. For 2D-H, $d_{wall} = a - d_{pore}$;[25] for 3D-FC, $d_{wall} = \frac{\sqrt{2}}{2}a - d_{pore}$;[26] for 3D-CB, $d_{wall} = \frac{a}{3.0919} - \frac{1}{2}d_{pore}$, where 3.0919 is a constant representing the minimal surface area for the *Ia3d* space group; for 3D-BC, $d_{wall} = \frac{\sqrt{3}}{2}a - d_{pore}$.[26] The obtained BET surface area, pore diameter and wall thickness of the mesoporous Nafion were calculated and are listed in Table 2. Mesoporous Nafion with structure symmetry 3D-CB exhibits the highest BET surface area of 781 $m^2\ g^{-1}$. 3D-FC Nafion show lowest specific surface area of 447 $m^2\ g^{-1}$, which may be due to the low order of mesoporous structure as shown by SAXS (Figure 1).

The formation mechanism and interaction among Nafion molecules, SDAs and silica colloids were further studied by the *in situ* time-resolved synchrotron SAXS, using 2D-H structured Nafion as an example. In the initial stage of the self-assembly process, the SAXS signal is typical of a micellar solution with broad oscillation as a function of the scattering vector q as shown in Figure 4A. A broad peak centered around 0.06 $Å^{-1}$ occurs at t = 600 s, which is most likely resulted from scattering of associated unordered globular micelles of Nafion-silica nanoparticles.[27] The peak becomes more pronounced with the reaction time because of the stabilizing functions of Nafion ionomers, that is, further agglomeration and grain growth of silica nanoparticles will be inhibited.[28] As the hydrolysis of TEOS only takes a few minutes to complete in the P123 micellar solution,[15] shape evolution and formation of

2D-hexagonal phase would occur between P123 and Nafion-silica pairs. Then, the structure transforms from the unordered micelles directly to the ordered hexagonal structured phase in solution, and such transformation occurs at ~600 s. As shown in Figure 4A, the intensity of the Bragg peaks of (100) reflection (0.04 $Å^{-1}$) increase with time, while the intensity of the micellar peak (0.06 $Å^{-1}$) decrease. The continuous increase in the intensity of the (100) reflection reflects an increase in the amount of ordered phase. This indicates the transformation process from the spherical micelles to the ordered and rod-shaped 2D-hexagonal structured phase. Moreover, the comparison of the diffractograms of the Nafion-silica composite taken at 100 s and 3000 s shows the evolution of the Bragg peaks of the hexagonal structure in solution (Figure 4B). The silica nanoparticle colloid that is attached both at Nafion ionomers and P123 expands the Nafion ordered arrays, and creates an electrostatic-induced reorientation of sulfonic groups towards the ordered silica-P123 micelles. Through cooperative hydrogen bonding self-assembly of the Nafion-silica pairs and P123, highly 2D-H ordered mesoporous structure is formed. The *in situ* time-resolved synchrotron SAXS results on the 2D-H Nafion-silica also imply that Nafion-silica with different mesoporous structure symmetries can be achieved by adjusting the reagents ratio and employing structure directing agents, SDAs with different ether blocks.[29]

Based on the in-situ time-resolved SAXS data, we proposed the process of the silica-mediator assisted formation of mesoporous Nafion membrane (see Figure 5 for the typical 2D-H structured Nafion). In the initial stage, the presence of acidic HCl

solution initiates and promotes the hydrolysis of TEOS, forming protonated and positively charged silica particles that play the role as bonding sites between Nafion ionomers and the SDAs, *i.e.*, P123 in this case. Driven by the electrostatic forces between the positively charged silica nanoparticles and the negatively charged SO_3^- function groups of Nafion ionomers, self-assembly of Nafion and silica nanoparticles occurs instantaneously, forming Nafion-silica pairs. Then, the Nafion-silica pairs will anchor to the ether block of the SDAs through hydrogen bonding. Nafion ionomers attached to the silica nanoparticles will stabilize the silica nanoparticles, inhibiting the agglomeration and grain growth of silica nanoparticles and forming ordered and mesoporous structured phase. Based on the time-resolved synchrotron SAXS (Fig.4A), the transformation from random micelles to ordered mesoporous phase occurs at ~600 s. Highly ordered and mesoporous Nafion ionomers are obtained after removal of both SDAs and silica mediators. The resulted mesoporous orientation would lead to the increasing exposure of sulfonic groups to the hydrophilic phase and form highly ordered proton transporting channels, promoting fast proton conduction process.[30]

Besides, the formation of ordered mesoporous Nafion-silica composites depends on the Nafion to silica ratio. Figure 6 shows the synchrotron SAXS profiles of 2D-H Nafion-silica powders with different contents of Nafion, measured at room temperature. The main (100) reflection was red-shifted from 0.053 $Å^{-1}$ to 0.067 $Å^{-1}$ when the Nafion increased from 10 % to 50 %, that is, the d_{100} spacing value reduced from 11.8 nm to 9.3 nm, respectively. When the Nafion content increased to 70 %, the silica became disordered and mesoporous Nafion-silica structure could not be

obtained. The increase in the content of Nafion would decrease the degree of order since the intensive interplay of amphipathic Nafion molecules with the silica-P123 micelles may significantly interrupt the self-assembly procedure of ordered silica-SDAs framework.[30] Nafion molecules would cover on the surface of silica colloids, forming Nafion-silica pairs because of self-assembly between the positively charged silica and the negatively charge Nafion ionomer by the electrostatic force. With the increase of the Nafion ionomers, the increasing polymer network would interrupt the assembly of silicate species to the PEO groups of the amphiphile and impedes the phase separation. Excess Nafion ionomers would interact with the P123, interrupting the formation of ordered and mesoporous phase in the Nafion-silica-P123 precursor solution. Thus, in the present study, the amount of Nafion in the Nafion-silica composites was controlled to 10 wt%.

3.2 Fuel cell performance of mesoporous Nafion membranes

To assess the hydrogen gas permeability of the mesoporous Nafion membranes, the hydrogen crossover current density was measured and the results are given in Table 2. Hydrogen crossover currents are in the range of 0.85 mA cm^{-2} to 1.54 mA cm^{-2} for mesoporous Nafion membranes, which is slightly higher than 0.69 mA cm^{-2} measured on pristine Nafion 112 membrane. This indicates that the detrimental effect of the presence of ordered mesoporous channels on the gas permeability of mesoporous Nafion membrane is relatively low, indicating the applicability of the mesoporous Nafion membranes synthesized in this study as PEMs for fuel cells.

High proton conductivity is an important requirement of PEMs for fuel cells. Proton conductivities of mesoporous Nafion membrane samples were measured *in situ* during the fuel cell operation by electrochemical impedance spectroscopy at 60 ^{o}C under different RH and the results are summarized in Table 2. The proton conductivity of mesoporous Nafion shows a very low sensitivity to the change in RH. For example, the proton conductivity for Nafion membranes with 2D-H structure is 0.08 Scm^{-1} at 100 % RH, similar to 0.072 Scm^{-1} measured on Nafion 112 membrane, but slightly lower than 0.1 Scm^{-1} reported on Nafion 115 membranes under 100% RH at 30 ^{o}C.[31] When the RH is reduced to 40%, the proton conductivity of 2D-H Nafion membrane is 0.062 Scm^{-1}, a reduction of 22.5%. In contrast, the proton conductivity of conventional Nafion 115 is 0.0042 Scm^{-1} at 40% RH, a reduction of 95.8% as compared to the value measured at 100% RH.[31] Most important, under 0 % RH, the proton conductivity of mesoporous Nafion is in the range of 1.9× 10^{-2} Scm^{-1} to 3.8 × 10^{-2} Scm^{-1}. Consequently, the most significant benefit of the mesoporous Nafion with different structural symmetries is the substantially enhanced proton conductivity at reduced RH.

Figure 7 is the polarization and power output performance of cells with mesoporous Nafion and Nafion 112 membranes, measured at 60 ^{o}C under various RH conditions. The open circuit voltage of all five Nafion membranes was in the range of 0.95 - 0.98 V. The polarization performance of cells with mesoporous Nafion membranes is considerably higher than that of the cells with pristine Nafion membrane, particularly under reduced RH. For example, under 60 % RH, the power

density of the cells with 2D-H, 3D-CB, 3D-BC, and 3D-FC Nafion membranes is 362 mW cm^{-2}, 224 mW cm^{-2}, 185 mW cm^{-2}, and 203 mW cm^{-2}, higher than 115 mW cm^{-2} obtained on Nafion 112. The cell with 2D-H Nafion membrane produced the highest power output.

The peak power density of cells with 2D-H, 3D-BC, 3D-CB and 3D-FC mesoporous Nafion membranes shows a very different dependence on RH, as compared to the cell with pristine Nafion 112 (Figure 7f). The peak power density of Nafion 112 reduced linearly with the decrease in RH. At 100 % RH, the power density of the Nafion membrane cell is 228 mW cm^{-2} and decreases to 77 mW cm^{-2} when the RH is reduced to 40%, a 66.2% reduction in power output. The significant reduction in power output of Nafion 112 membrane cell is clearly due to the fact that the proton conductivity of Nafion membranes decreases significantly with decreasing RH.[32-34] In the case of the cells with mesoporous Nafion membranes, dependence of the power density on RH follows a S-type curve. The S-type dependence of the polarization performance on the RH has also been observed on functionalized mesoporous silica cells.[35, 36] The S curves indicate that the power output of the mesoporous Nafion membrane cells is less sensitive to the change in RH, which is likely due to the fact that ordered mesoporous channels have a much better water retention ability as compared to the random nanostructures associated with pristine Nafion membranes. The less sensitivity of the power performance of the cells to RH is an important factor for practical operations as this will allow more stable power output under conditions of RH fluctuation. The cell with 2D-H mesoporous Nafion membrane produces the

best performance; 414 mW cm^{-2} under 100% RH and 310 mW cm^{-2} under 40% RH. Fukuda et al[37] showed that variation of power density with the RH is consistent with the tendency of the amount of H_2O adsorbed on the Nafion membrane. Thus the low sensitivity or dependence on RH of mesoporous Nafion membrane cells is most likely due to the water capillary condensation effect of the mesoporous structure at reduced relative humidity. On the other hand, the hydrophilic clusters of Nafion 112 membrane with $-SO_3H$ group have to adsorb large amount of water in order to form the continuous proton transportation channels, resulting in high dependence on external humidification and RH.[38] Consequently, the highest performance of 2D-H mesoporous Nafion based fuel cell indicates the effectiveness of the highly ordered hexagonal cylinders structure for water retention.

The stability of mesoporous Nafion and Nafion 112 membrane based fuel cells was evaluated as a function of RH. Figure 8 shows the cell voltage, measured at a constant discharge current density of 100 mA cm^{-2} and 60 ^oC under different RH. The RH decreased from 100 % to 0 % in decrements of 20 % every 20 h. For the 2D-H Nafion cell, the initial voltage is ~0.68 V at 100% RH and 80% and is more or less stable. When RH descended to 60%, the cell voltage slightly dropped to 0.65 V. The most interest observation is the stable performance observed on the 2D-H Nafion membrane cell under 0% RH (i.e., anhydrous conditions). The initial cell voltage was 0.56 V and decreased to 0.47 V after 20 h of operation. This demonstrates that highly ordered mesoporous Nafion membrane is capable to operate under anhydrous conditions clearly due to the extraordinary water retention ability of the ordered

mesoporores. This is consistent with the high proton conductivities of mesoporous Nafion at 0% RH (1.9×10^{-2} - 3.8×10^{-2} Scm^{-1} at $60^{o}C$, Table 2). On the contrary, the cells of conventional Nation 112 membranes can only operate at high RH of 100 and 80%. When the RH decreased to 60%, the initial cell voltage was 0.54 V, and dropped very quickly to zero in 55 min (Fig.8B). Under anhydrous conditions (e.g., 0% RH), the cell ceased to operate within 20 min (Fig.8C). The rapid failure of cells based on conventional Nafion membranes under reduced RH clearly indicates the poor water retention properties of conventional Nation membranes with random nanostructures.[9] The stable cell performance of cells with mesoporous Nafion membrane under low RH and anhydrous conditions confirms again an extraordinarily high water retention capacity of ordered mesoporous structured Nafion membranes, most likely due to the effective capillary condensation effect in ordered mesopores as discussed above.

4 Conclusions

The formation of ordered and mesoporous structured phase in solution in Nafion-silica-SDA precursor solutions was studied for the first time using *in situ* time-resolved synchrotron SAXS technique. The results clearly demonstrate the formation of highly ordered and mesoporous Nafion-silica-SDA (P123 was used as the SDA in this study) structures in the presence of silica colloidal mediator. Such formation of ordered mesoporous phase in solution is critical for the formation of highly ordered mesoporous Nafion membrane with controlled structure symmetry from 2D-H, 3D-FC, 3D-CB to 3D-BC.

The present study reported an effective synthesis strategy to introduce and control the mesoporous structure symmetry of PFSA-based membranes such as Nafion. The ability to introduce and control the mesoporous structure symmetries is important in the development of highly effective and functional PEMs for fuel cells. The results demonstrate that highly ordered mesoporous Nafion membrane have superior proton conductivity and enhanced electrochemical performance as compared to the pristine Nafion. For example, the proton conductivity for Nafion membranes with 2D-H structure is 0.08 Scm^{-1} at 100 % RH and decreases to 0.062 Scm^{-1} when RH is 40%, a reduction of only 22.5%. In contrast, the reduction in the proton conductivity of conventional Nafion membranes is 95.8% at 40% RH as compared to the value measured at 100% RH.[31] Most importantly, the present study also demonstrated for the first time that mesoporous structured Nation membranes based cells can be operated under 0% RH, i.e., anhydrous conditions, an unique advantage over conventional Nation membranes. Among the ordered mesoporous structures, 2D hexagonal exhibit the highest proton conductivity and the highest cell performance due to meso-morphology and long-range periodicity which is facile for proton transport and mass transfer.

Acknowledgment

This work is financially supported by the National Natural Science Foundation of China (61274135, 51272200), Program for New Century Excellent Talents in University (NCET-12-0911), Australian Research Council *Discovery Project funding*

scheme (project number: DP120102325 and DP120204932) and the Fundamental Research Funds for the Central Universities (WUT: 2013-IV-037, 2013-II-011). The time-resolved synchrotron SAXS measurements were carried out on the SAXS beamline at the Australian Synchrotron, Victoria, Australia.

References:

1. Y. Sone, P. Ekdunge and D. Simonsson, *J. Electrochem. Soc.*, 1996, **143**, 1254-1259.
2. M. N. Silberstein, P. V. Pillai and M. C. Boyce, *Polymer*, 2011, **52**, 529-539.
3. R. Solasi, X. Y. Huang and K. Reifsnider, *Mechanics of Materials*, 2010, **42**, 678-685.
4. H. W. Zhang and P. K. Shen, *Chem. Soc. Rev.*, 2012, **41**, 2382-2394.
5. L. Rubatat and O. Diat, *Macromolecules*, 2007, **40**, 9455-9462.
6. S. S. Jang, V. Molinero, T. Çağın and W. A. Goddard, *The Journal of Physical Chemistry B*, 2004, **108**, 3149-3157.
7. K. Schmidt-Rohr and Q. Chen, *Nat. Mater.*, 2008, **7**, 75-83.
8. M.-H. Kim, C. J. Glinka, S. A. Grot and W. G. Grot, *Macromolecules*, 2006, **39**, 4775-4787.
9. O. Diat and G. Gebel, *Nature materials*, 2008, **7**, 13-14.
10. J. L. Lu, S. F. Lu and S. P. Jiang, *Chem. Commun.*, 2011, **47**, 3216-3218.
11. J. Lu, H. Tang, C. Xu and S. P. Jiang, *J. Mater. Chem.*, 2012, **22**, 5810-5819.
12. G. Armatas, C. Salmas, M. Louloudi, G. Androutsopoulos and P. Pomonis, *Langmuir*, 2003, **19**, 3128-3136.
13. S. Dourdain and A. Gibaud, *Applied Physics Letters*, 2005, **87**, 223105-223105-223103.
14. J. Li, H. Tang, L. Chen, R. Chen, M. Pan and S. P. Jiang, *Chemical Communications*, 2013, **49**, 6537-6539.
15. S. Manet, J. Schmitt, M. Imperor-Clerc, V. Zholobenko, D. Durand, C. L. P. Oliveira, J. S. Pedersen, C. Gervais, N. Baccile, F. Babonneau, I. Grillo, F. Meneau and C. Rochas, *J. Phys. Chem. B*, 2011, **115**, 11330-11344.
16. F. Michaux, N. Baccile, M. Imperor-Clerc, L. Malfatti, N. Folliet, C. Gervais, S. Manet, F. Meneau, J. S. Pedersen and F. Babonneau, *Langmuir*, 2012, **28**, 17477-17493.
17. Y. Wan and D. Y. Zhao, *Chem. Rev.*, 2007, **107**, 2821-2860.
18. D. Zhao, J. Feng, Q. Huo, N. Melosh, G. H. Fredrickson, B. F. Chmelka and G. D. Stucky, *Science*, 1998, **279**, 548-552.
19. J. Fan, C. Yu, F. Gao, J. Lei, B. Tian, L. Wang, Q. Luo, B. Tu, W. Zhou and D. Zhao, *Angewandte Chemie*, 2003, **115**, 3254-3258.
20. D. Zhao, Q. Huo, J. Feng, B. F. Chmelka and G. D. Stucky, *Journal of the American Chemical Society*, 1998, **120**, 6024-6036.
21. X. Liu, B. Tian, C. Yu, F. Gao, S. Xie, B. Tu, R. Che, L.-M. Peng and D. Zhao, *Angewandte Chemie International Edition*, 2002, **41**, 3876-3878.
22. G. Gebel, P. Aldebert and M. Pineri, *Macromolecules*, 1987, **20**, 1425-1428.
23. M. Fujimura, T. Hashimoto and H. Kawai, *Macromolecules*, 1981, **14**, 1309-1315.

24. Y. Meng, D. Gu, F. Zhang, Y. Shi, L. Cheng, D. Feng, Z. Wu, Z. Chen, Y. Wan, A. Stein and D. Zhao, *Chemistry of Materials*, 2006, **18**, 4447-4464.
25. E.-B. Cho, S. Yim, D. Kim and M. Jaroniec, *Journal of Materials Chemistry A*, 2013, **1**, 12595-12605.
26. D. Carmona, F. Balas, A. Mayoral, R. Luque, E. P. Urriolabeitia and J. Santamaria, *Chemical Communications*, 2011, **47**, 12337-12339.
27. K. Flodstrom, C. V. Teixeira, H. Amenitsch, V. Alfredsson and M. Linden, *Langmuir*, 2004, **20**, 4885-4891.
28. H. Tang, Z. Wan, M. Pan and S. P. Jiang, *Electrochem. Commun.*, 2007, **9**, 2003-2008.
29. Y. Wan and Zhao, *Chemical Reviews*, 2007, **107**, 2821-2860.
30. L. Chen, H. Tang and M. Pan, *International Journal of Hydrogen Energy*, 2012, **37**, 4694-4698.
31. J. Zeng, Y. H. Zhou, L. Li and S. P. Jiang, *Phys. Chem. Chem. Phys.*, 2011, **13**, 10249-10257.
32. T. A. Zawodzinski, T. E. Springer, J. Davey, R. Jestel, C. Lopez, J. Valerio and S. Gottesfeld, *J. Electrochem. Soc.*, 1993, **140**, 1981-1985.
33. X. M. Yan, P. Mei, Y. Z. Mi, L. Gao and S. X. Qin, *Electrochem. Commun.*, 2009, **11**, 71-74.
34. F. N. Buchi and G. G. Scherer, *J. Electrochem. Soc.*, 2001, **148**, A183-A188.
35. J. Zeng, P. K. Shen, S. F. Lu, Y. Xiang, L. Li, R. De Marco and S. P. Jiang, *J. Membr. Sci.*, 2012, **397**, 92-101.
36. J. Zeng and S. P. Jiang, *Journal of Physical Chemistry C*, 2011, **115**, 11854-11863.
37. S. Fukada, K. Ohba and A. Nomura, *Energy Conversion and Management*, 2013, **71**, 126-130.
38. G. S. Hwang, M. Kaviany, J. T. Gostick, B. Kientiz, A. Z. Weber and M. H. Kim, *Polymer*, 2011, **52**, 2584-2593.

Table 1. Peak position q, d spacing and lattice parameter a for the mesoporous Nafion-silica and mesoporous Nafion membranes.*

Space	Mesoporous Nafion-silica			Mesoporous Nafion		
symmetries	q / Å^{-1}	d / nm	a / nm	q / Å^{-1}	d / nm	a / nm
2D-H	0.065	9.7	11.2	0.068	9.2	10.6
3D-FC	0.064	9.8	13.9	0.051	12.3	17.4
3D-CB	0.071	8.8	21.6	0.058	10.8	26.7
3D-BC	0.053	11.8	20.6	0.051	12.3	21.3

*Notation: $d = \frac{2\pi}{q}$; lattice parameter for 2D-H, $a = \frac{2}{\sqrt{3}} d_{(100)}$; lattice parameter for 3D-FC, $a = \sqrt{2} d_{(111)}$; lattice parameter for 3D-CB, $a = \sqrt{6}\, d_{(211)}$; lattice parameter for 3D-BC, $a = \sqrt{3}\, d_{(110)}$;

Table 2. BET surface area S_{BET}, pore diameter d_{pore}, wall thickness d_{wall} and hydrogen crossover current density j, the proton conductivity σ of diverse mesoporous Nafion and pristine Nafion.

Type of Nafion	S_{BET}	d_{pore}	d_{wall}	j	σ / × 10^{-2} Scm^{-1} (60 °C)		
	(m^2 g^{-1})	(nm)	(nm)	(mA cm^{-2})	0 % RH	40 % RH	100 % RH
2D-H Nafion	609	5.3	2.7	1.15	3.8	6.2	8.0
3D-FC Nafion	447	3.8	8.5	0.85	2.4	5.0	7.0
3D-CB Nafion	781	3.8	7.0	1.54	1.9	3.3	7.2
3D-BC Nafion	554	4.7	10.3	0.88	2.7	4.4	6.9
Pristine Nafion	—	—	—	0.69		0.42*	10*

*Measured on Nafion 115 at 30°C.[31]

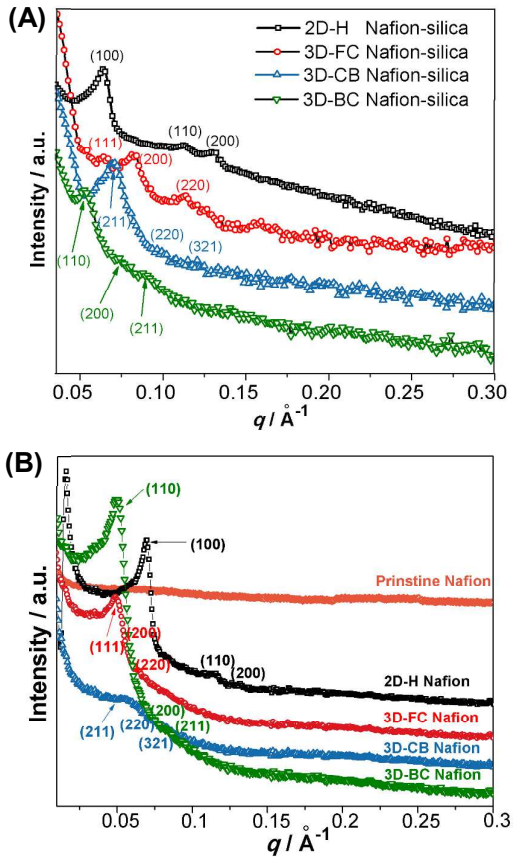

Figure 1. SAXS spectra of (A) mesoporous Nafion-silica composites with 2D-H, 3D-FC, 3D-CB and 3D-BC mesoporous structures after removal of the structure directing agents (SDAs), and (B) corresponding mesoporous Nafion membranes after removal of silica. SAXS pattern of pristine Nafion 112 membrane is shown in B.

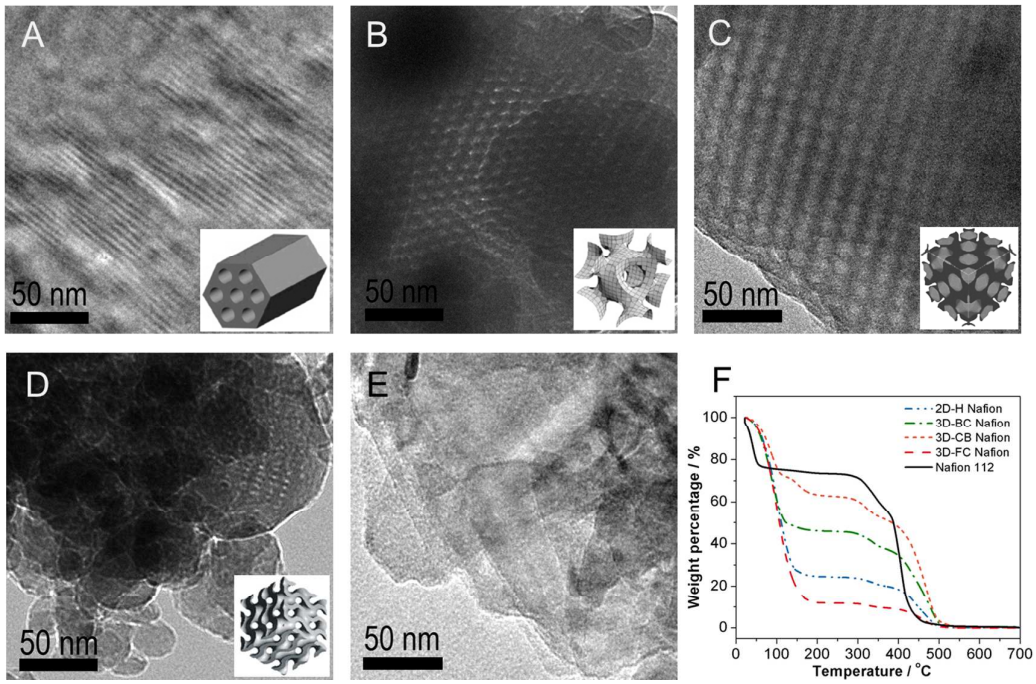

Figure 2. TEM morphologies of mesoporous Nafion with (A) 2D hexagonal (2D-H, *P6mm*) in [110] direction, (B) 3D body-centered (3D-BC, $Im\overline{3}m$) in [111] direction, (C)3D face-centered (3D-FC, $Fm\overline{3}m$) in [100] direction, (D) 3D cubic-bicontinuous (3D-CB, $Ia\overline{3}d$) mesoporous structures in [311] direction and (E) pristine Nafion membrane.[14] TGA profiles of mesoporous Nafion membranes with different space symmetries and pristine Nafion membrane as the control group are shown in (F).

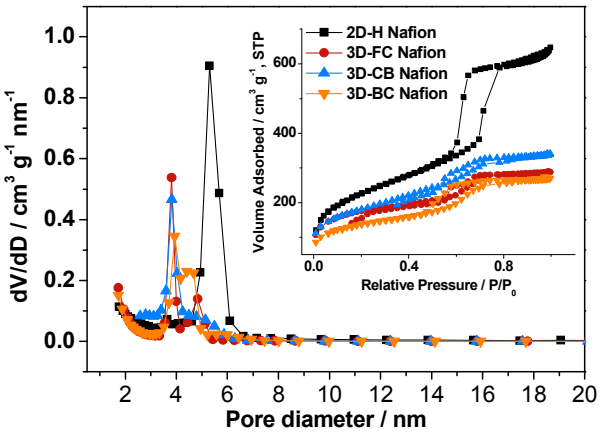

Figure 3. Nitrogen sorption isotherms and pore size distribution of mesoporous Nafion membranes with different structure symmetries.

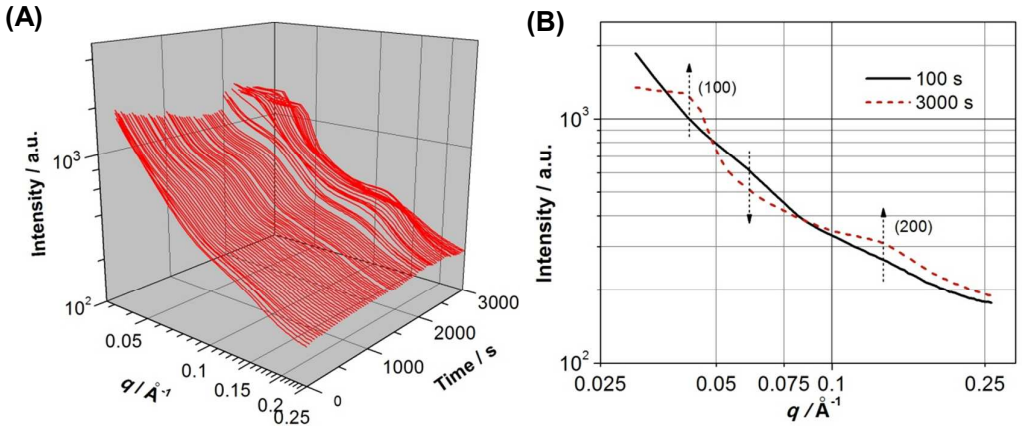

Figure 4. (A) Time-resolved synchrotron SAXS diffractograms and (B) 100 s and 3000s SAXS curves of the silica colloids-mediated synthesis of 2D hexagonal mesoporous Nafion-silica composite (10 wt% Nafion) in P123 + HCl + Nafion ionomers + TEOS solution without stirring.

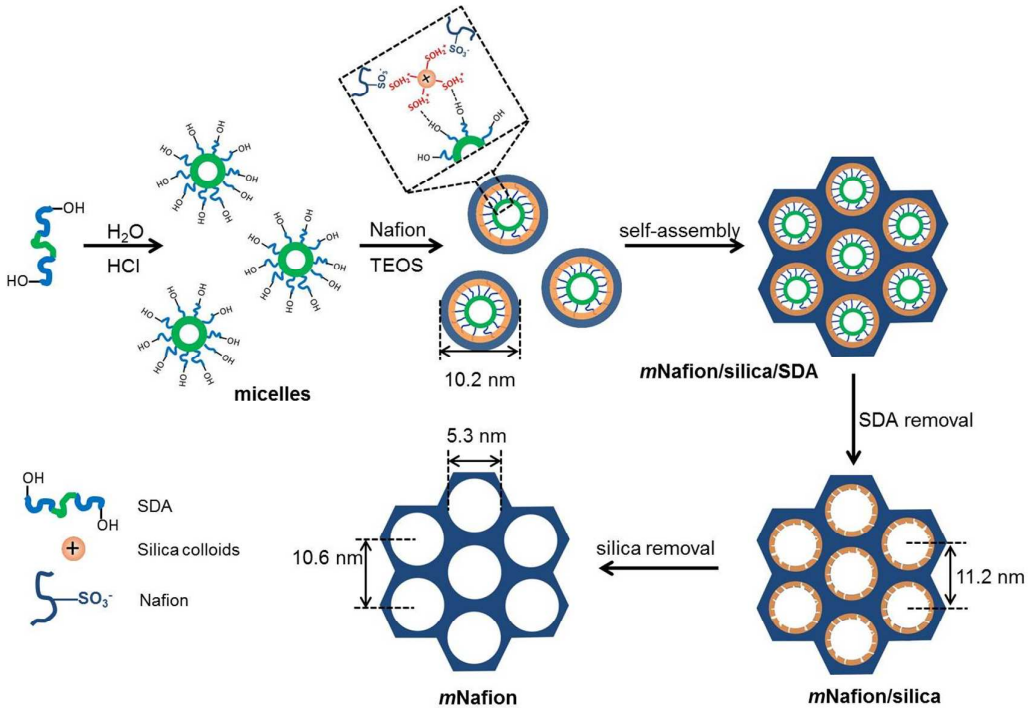

Figure 5. Schematic of a surfactant-directed and soft template method with the assistance of silica colloidal mediator for the formation of mesoporous Nafion (2D-H structured Nafion was selected as a representative). The transformation from the random micelles to the ordered hexagonal structural phase in solution occurs at ~600 s.

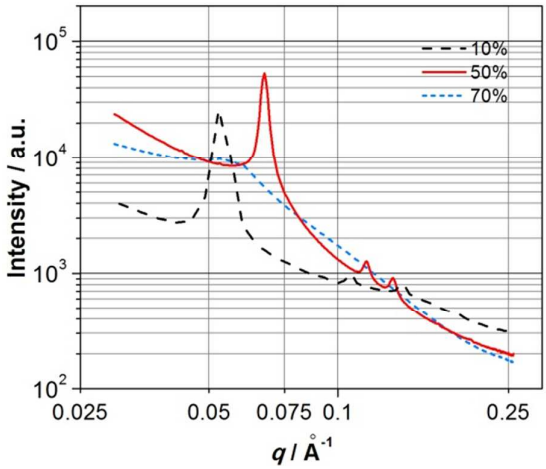

Figure 6. Synchrotron SAXS profiles of 2D hexagonal Nafion-silica powders with Nafion content of 10 %, 50 % and 70 %, measured at room temperature.

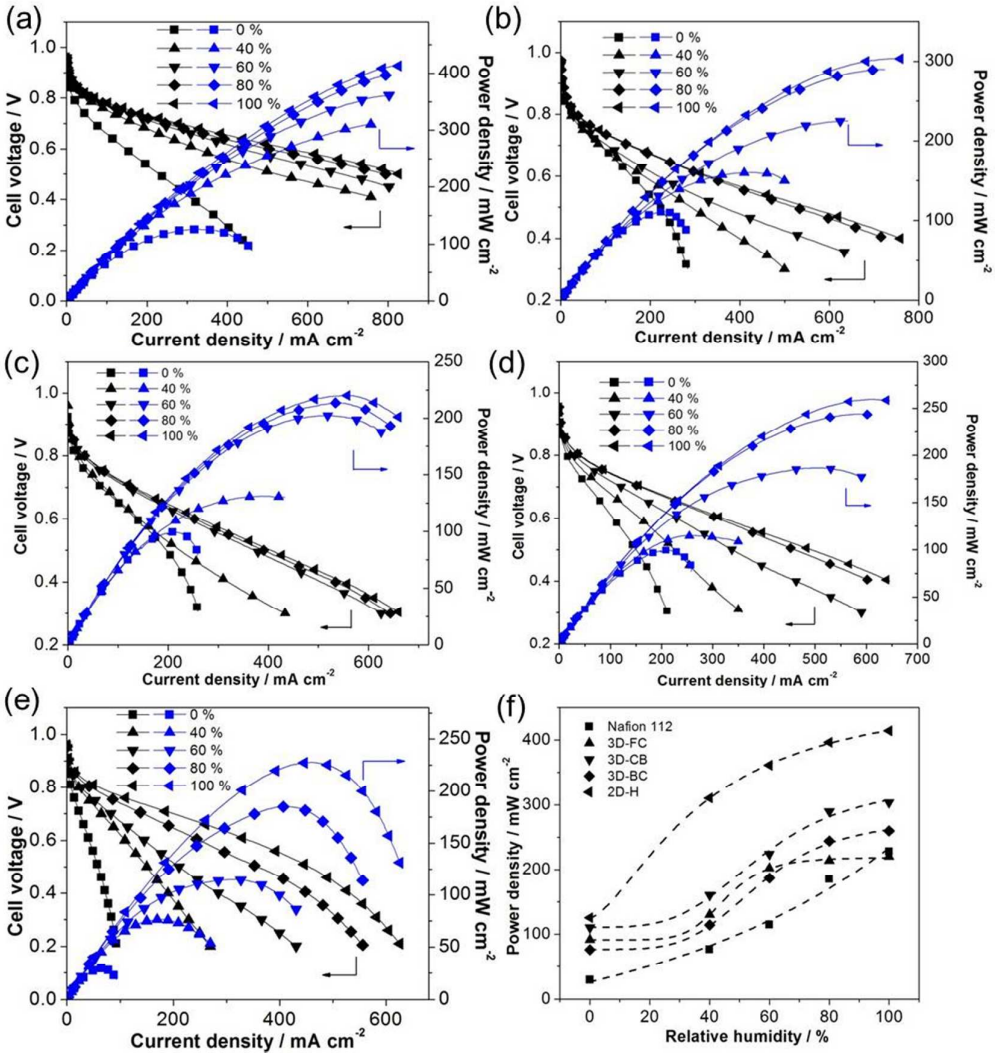

Figure 7. Polarization and power output of cells, measured at 60 ^{o}C, H_2/O_2 with (a) 2D-H Nafion membrane, (b) 3D-CB Nafion membrane, (c) 3D-FC Nafion membrane, (d) 3D-BC Nafion membrane, (e) Nafion 112 membrane. Peak power density of mesoporous Nafion membranes against various relative humidity at 60 ^{o}C was given in (f).

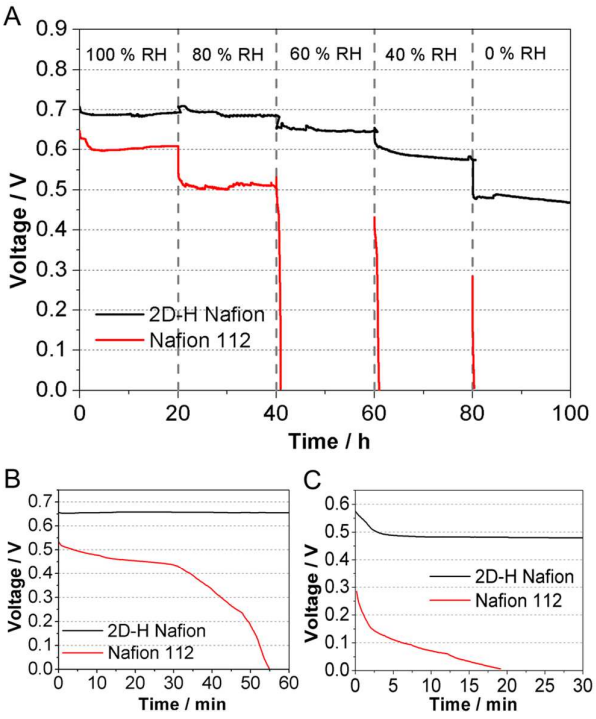

Figure 8. (A) Plots of cell voltage measured under different RH levels for 2D-H Nafion and Nafion 112 membrane based fuel cells. (B) and (C) are the enlarged portion of the voltage curves of the cells under 60 % RH and 0 % RH, respectively. The cells were tested at 60 ^{o}C in H_2/O_2 under a constant discharge current density of 100 mA cm^{-2}.

Graphic abstract

Highly-ordered mesoporous-structured Nafion membranes are synthesized by a new soft template method assisted with silica colloidal mediator for fuel cells.